Asian Journal of Chemistry; Vol. 36, No. 5 (2024), 1119-1125

ASIAN JOURNAL OF CHEMISTRY

https://doi.org/10.14233/ajchem.2024.31270

Green Synthesis and Characterization of CaO Nanoparticles using Hen Eggshells and its Impact on Biomass Concentration, Chlorophyll-a and Lipid Content of *Chlorella* sp.

Richa Pahariya[1], Abhishek Chauhan[2,*], Anuj Ranjan[2], Vinay Mohan Pathak[3], Hardeep Singh Tuli[4], Moyad Shahwan[5,6], Rupesh Kumar Basniwal[7], Sumant Upadhyay[8] and Tanu Jindal[2,*]

[1]Amity Institute of Environmental Sciences, Amity University, Noida-201313, India
[2]Amity Institute of Environmental Toxicology Safety and Management, Amity University, Noida-201313, India
[3]Pritam International Private Ltd, Roorkee-247661, India
[4]Department of Bio-Sciences and Technology, Maharishi Markandeshwar Engineering College, Maharishi Markandeshwar (Deemed to Be University), Mullana, Ambala-133207, India
[5]Department of Clinical Sciences, College of Pharmacy and Health Sciences, Ajman University, Ajman 346, United Arab Emirates
[6]Centre of Medical and Bio-Allied Health Sciences Research, Ajman University, Ajman 346, United Arab Emirates
[7]Amity Institute of Nanotechnology, Amity University, Noida-201313, India
[8]Amity Institute of Advanced Research and Studies (M&D), Amity University, Noida-201313, India

*Corresponding authors: E-mail: akchauhan@amity.edu; tjindal@amity.edu

Received: 17 January 2024; *Accepted*: 26 March 2024; *Published online*: 30 April 2024; AJC-21618

Biodegradable wastes *e.g.* the outer cover of a boiled hen egg generally haphazardly discarded by humans in different locations of the country and generates problems for the local creatures. Although different researchers reported different methods to utilize the waste through the nanotechnological approach. Here, green synthesis of calcium oxide (CaO) nanoparticles from the hen eggshells was carried out and characterized them by using X-ray diffraction (XRD), scanning electron microscope (SEM), energy dispersive X-ray (EDX) analysis, Fourier transform infrared spectroscopy (FTIR) and ultraviolet-visible spectrophotometer (UV). Further application of the synthesized nanoparticles was done on *Chlorella* sp. to investigate the impact on algal growth, lipid and chlorophylls. Synthesized CaO nanoparticles were applied in different concentration (0, 10, 20 and 30 mg L^{-1}) and readings were monitored for 20 days. The highest biomass concentration 242.56 mg L^{-1} was achieved for the nanoparticle concentration of 20 mg L^{-1} and the lipid content increased up to 35.71% in 20 mg L^{-1}. These results pave the way for enhanced algal biofuel production.

Keywords: Green synthesis, Calcium oxide nanoparticle, Phylogenetic analysis, Microalgae response, Biofuel production.

INTRODUCTION

Green synthesis of nanoparticles has become a viable alternative to traditional chemical processes in recent times [1]. Typically, the chemical techniques employed tend to be costly and involve the utilization of hazardous and harmful chemicals. Chemical procedures typically involve multiple chemical species or compounds that have the potential to increase particle reactivity and toxicity as well as represent a threat to the public health and the environment [2]. In the arena of sustainable synthesis, green synthesis stands out as a bottom-up method corresponding to chemical reduction. The field of nanoscience aims to result in the creation of environmentally safe nanoparticles and has gained broad acceptance within the realm of nanotechnology [3]. The biosynthetic pathway offers a secure, biocompatible, eco-friendly method for producing nanoparticles, suitable for biomedical purposes [4-6]. This process involves utilizing plants and microorganisms, including fungi, algae, bacteria, various plant parts and waste materials, to synthesize a diverse range of nanoparticles, it innovatively swaps out costly chemical reducing agents facilitating the creation of nanoparticles. Several researchers synthesized silver nanoparticles (Ag NPs) from a microalgae *Planophila laetevirens*, the synthesized nanoparticles are beneficial to medicine and industries [7].

Harnessing the power of biological entities holds immense promise for advancing nanoparticle production methods. Synthesized particles from green route are found very beneficial as pharmaceuticals, biosensors, medicinal purposes, catalysts, biofuel and pharmaceuticals [8-10]. The addition of nanoparticles in biofuel feedstock to combat the energy scarcity problem has attracted many researchers due to their economical and sustainable approaches [11]. The best biofuel substitute, according to many, is biodiesel made from microalgae considering it is affordable, non-food based, pollution free and environmentally compassionate. Numerous investigations have been conducted to improve the generation of biofuels from microalgae by altering their dietary needs. Due to the strong potential for biofuel generation and the presence of important fats and polysaccharides, microalgae have been selected [12,13].

Furthermore, microalgae exhibit several advantages, including elevated lipid accumulation, accelerated development and the ability to thrive under a variety of odd growth situations [14]. Calcium is crucial for sustaining cellular function and is a fundamental component of plant tissues [15] and microalgae [16]. The experimental investigation of microalgae cultivation using nanoparticles containing silica and calcium compounds demonstrated a significant enhancement in microalgae cellular growth. This improvement occurred without adverse effects on harvesting efficiency or biofuel production from vegetable oil. In the study it was found that a reduced level of calcium ions (Ca^{2+}) facilitated the removal of chemical oxygen demand (COD) and nutrients by stimulating the growth of microalgae, resulting in an increase in chlorophyll-a concentration [17]. While studying Ca^{2+}, it was observed that single cell dry weight was increased in microalgae *Auxenochlorella protothecoides* UTEX234. The analysis of cellular components revealed a substantial decrease in both carbohydrate and total protein content, accompanied by a notable 158% increase in lipid content [18].

The impact of CaO nanoparticles on plants has also been thoroughly investigated. The green synthesized ZnO + CaO from *Nigella sativa* seeds gave favourable results in shoot length, number of shoots, number of roots, yield/plant, fruit weight and leaf area of tomato plant at the concentration of 50 ppm [19]. Affordable and eco-conscious calcium oxide nanoparticles (CaO NPs) were produced through environmentally friendly means by utilizing the aqueous extract derived from *Tulbaghia violacea* bulbs [20]. Similarly, CaO NPs were synthesized by utilizing the aqueous stem extract of *Cissus quadrangularis* [21]. Present study focused on synthesis of CaO NPs from waste material (hen eggshells) and its application to produce third generation biofuel. CaO nanoparticles were characterized by various techniques. Furthermore, the synthesized CaO NPs were investigated on *Chlorella* sp. for effects on algal growth, lipid, and chlorophylls.

EXPERIMENTAL

For this study, the reagents and chemicals were acquired from the reputed commercial sources. Chloroform ($CHCl_3$) with a purity of ≥ 99.80% and methanol (CH_3OH) were purchased from Fischer Scientific, India. BG-11 Broth (Blue-Green medium) was procured from Hi-media, India, whereas hen's eggshells were collected from the local market.

Microalgal culture: The microalga *Chlorella* sp. BDUG 20021 was obtained from the National Facility for Marine Cyanobacteria, Bharathidasan University, Tiruchirappalli, India. For the inoculation, a sterile culture BG 11 medium was made at pH 7.1. The isolate was then identified by PCR sequencing of the whole 16S rRNA gene, based on molecular features. DNA was extracted using Gen Elute™ Bacterial Genomic DNA kit (Sigma-Aldrich, USA). The fundamental structurally conserved RNA of a small portion of eukaryotic cytoplasmic ribosomes is called 16S rRNA. These genes' sequence information is frequently utilized in molecular analyses to piece together the evolutionary history of organisms, particularly algae. One of the most widely utilized genes and a crucial marker for random PCR in environmental biodiversity screening is the small subunit (SSU) 16S rRNA gene. Using the genomic DNA as template and the primer pairs (F) TACTAGAAGGTTCGATTAGTC and (R) AGCAGGAAAAGAAACTA, the PCR amplification was carried out. The PCR process was carried out using a thermal schedule that included 3 min of initial denaturation at 94 ºC, 35 cycles of denaturation step at 94 ºC for 1 min, annealing at 50 ºC for 1 min and extension at 72 ºC for 2 min, followed by 7 min of final extension at 72 ºC. In order to exclude impurities, the PCR amplicon underwent purification and was further resolved on an agarose gel. The National Centre for Biotechnology (NCBI) used Blast software to align and analyze the sequencing data after the PCR product was sequenced in both directions. This allowed to identify the microalgae and its nearest neighbours [22]. The first 10 sequences were chosen and aligned by importing them into different alignment software programs based on the maximum identity score. ClustalW, The program MEGA 10 was used to create the phylogenetic tree, with the neighbour-joining strategy [23,24]. A 1000-replication bootstrap analysis was used to assess the stability within the clades of phylogenetic tree.

Formation of calcium oxide (CaO) nanoparticles from eggshells: The eggshells were collected from local supplier and washed with distilled water two to three times to remove any impurities. Following this, the shells were boiled for 20 min to eliminate the membrane inside. Once boiled, they were dried in an oven at 105 ºC. After drying, the shells were ground into a finer powder using a blender. Finally, the powdered eggshells were calcinated in a muffle furnace at 900 ºC for 4 h [25]. Heating of calcium carbonate (chemical nature of eggshell) at higher temperatures results into formation of CaO and CO_2. Carbon dioxide released into the atmosphere and remaining calcium oxide were further characterized.

Characterization: The X-ray diffraction analysis were carried out using a Philips XRD 3100 diffractometer (Philips Electronics Co., Eindhoven, Netherlands) with a moderate scanning speed of 0.3º/s across a 2θ range of 20-70º. The SEM and EDX analysis were conducted using a TESCAN Magna 200 eV-30 KV instrument, which allowed for the cross-sectional analysis, morphology assessment and elemental analysis specifically targeting Ca and O elements. The optical characteristics (UV-vis) of the specimens were assessed utilizing an Agilent

technologies Cary 60 UV-vis spectrophotometer, coupled with an integrating sphere accessory. Fourier transform infrared spectroscopy (FT-IR) analysis (Bruker Vertex 70 FTIR spectrophotometer with Platinum ATR instrument) in the 4000-400 cm^{-1} range was used to investigate the functional groups of the catalysts.

Algal growth with synthesized nano CaO: *Chlorella* sp. was grown in 250 mL Erlenmeyer flasks containing a total 100 mL volume of BG-11 medium and different concentrations of nano CaO in the photo-incubator at 25-30 ºC. The culture at 0, 10, 20, 30 mg L^{-1} was cultivated in 16 h or 8 h light and dark cycles under fluorescent white light with an intensity of 3-5 flux. To prevent adhering, the cultures were manually shaken by hand for three times a day. The experiment was carried out in triplicates.

Growth analysis: The microalgae's growth was assessed by measuring its optical density at 680 nm using a UV-visible spectroscope every 2 days over a span of 20 days. To calculate the biomass concentration, the microalgal biomass was collected through centrifugation and washed with double distilled water to eliminate impurities. Subsequently, the centrifuged pellets were dried in an oven set at 60 ºC until they achieved a stable weight. Once dried, the biomass was transferred to desiccators [26].

To calculate chlorophyll-a, an aliquot (1 mL) of microalgae culture was centrifuged three times at room temperature for 10 min at 6000 rpm. After three rinses with distilled water, the resulting pellets were re-suspended in 1 mL of methanol. The tubes were sealed and placed in a water bath at 60 ºC for 30 min to extract chlorophyll-a. Absorbance measurements were taken at 652, 665.2 and 750 nm and Porra's equation was used to determine the chl-a concentration in μg mL^{-1} [27].

Biomass concentrations and chlorophyll-a were calculated by using given equations:

$$\text{Biomass concentration} = \frac{\text{Weight (mg)}}{\text{Volume of culture (L)}}$$

$$\text{Chlorophyll-a} = 16.29\,(A_{665.2} - A_{750}) - 8.54\,(A_{652} - A_{750})$$

Extraction of lipids from *Chlorella* sp.: Microalgae lipids were extracted using a modified Bligh and Dyer method [28]. Dried and powdered microalgal biomass was dispersed in deionized water, then subjected to microwave pretreatment for 2 min at 540 W to disrupt cell walls. After cooling, chloroform and methanol were added and then the mixture was shaken vigorously for 4 h at room temperature. Water was subsequently added to facilitate the phase separation. After allowing the mixture to settle, the organic phase containing chloroform and lipids was carefully collected. The lipid content was determined using an equation:

$$\text{Lipid content (\%)} = \frac{\text{Mass of lipid (g)}}{\text{Mass of algae culture (g)}} \times 100$$

RESULTS AND DISCUSSION

A total of 193 ng of DNA was extracted from the given strain. Upon conducting 16S rRNA sequencing, it was determined that strain exhibits a similarity of 99.41% with *Chlorella* sp. The phylogenetic tree (Fig. 1) confirmed that given strain is *Chlorella* sp.

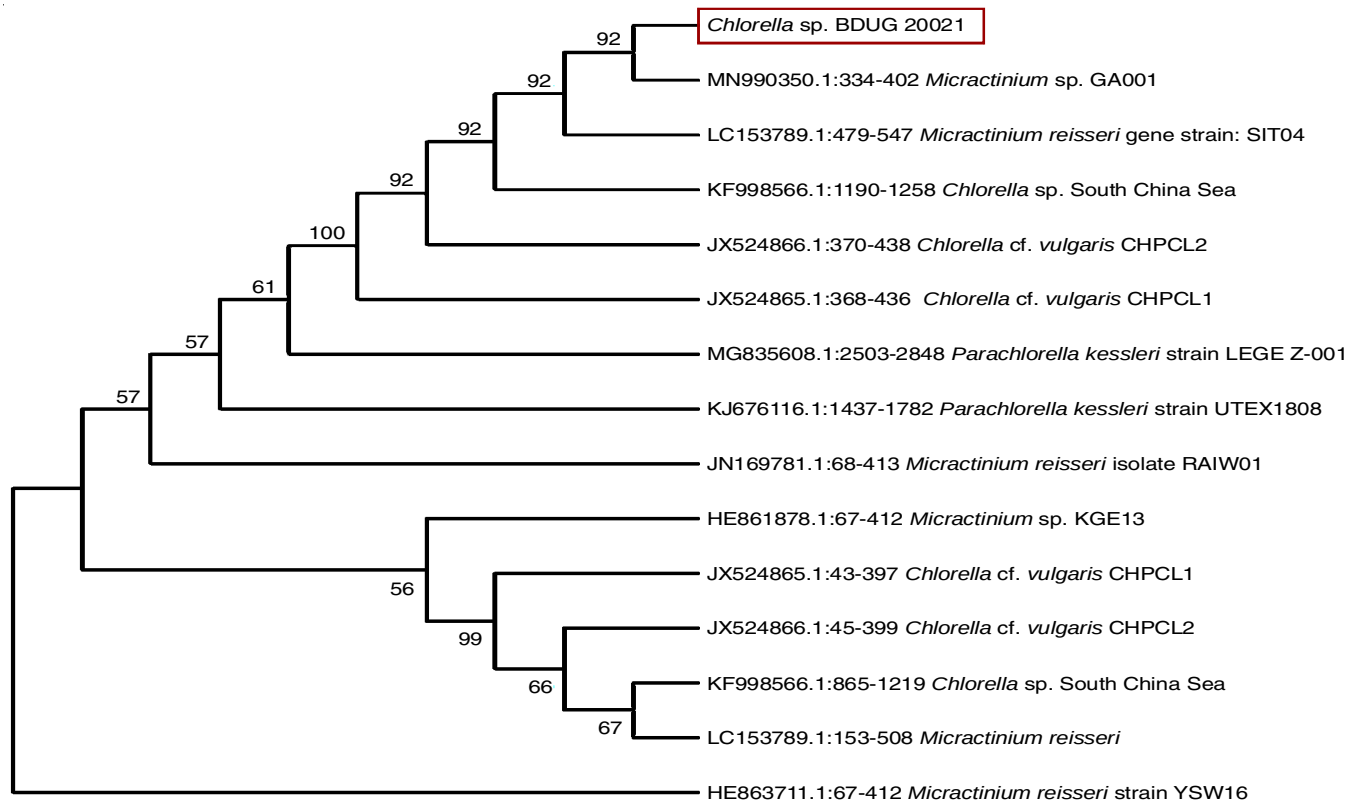

Fig. 1. Phylogenetic tree of the strain with its adjoining neighbours

XRD studies: Fig. 2 shows the X-ray diffraction (XRD) patterns of CaO nanoparticles. The obtained XRD results were compared with JCPDF card no. 37-1497, identifying peaks at 2θ = 33.67º, 39.07º, 52.22º and 67.03º corresponding to (*h k l*) values of (111), (200), (220) and (222), respectively. Additionally, the peaks of $Ca(OH)_2$ at 2θ = 55.90º, 59.37º, 69.03º and 77.00º were observed, with corresponding (*h k l*) values of (003), (200), (202) and (004), respectively. The results were found to be similar with reported literature [29]. The average crystallite size (D) of CaO nanoparticles was determined using the Debye-Scherrer's equation, given as follows:

$$D = \frac{K\lambda}{\beta\cos\theta}$$

where θ is the location of the diffraction peak's maximum and β = full width at half-maximum (in radians); K = 0.9, is defined as a shape factor.

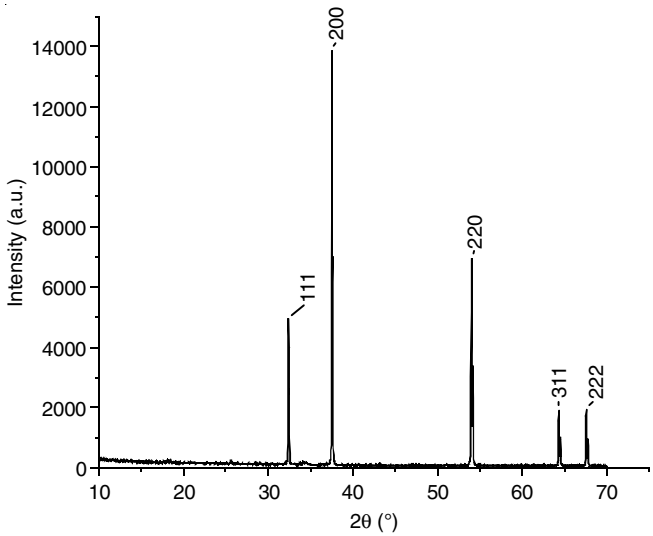

Fig. 2. X-ray diffraction (XRD) pattern of as-prepared CaO nanoparticles using hen eggshells

Morphological studies: FE-SEM was used to study the surface morphology of CaO NPs (Fig. 3). The images indicate the resultant CaO NPs had a porous structure (Fig. 3a) and were between 50 and 100 nm in size (Fig. 3b).

Using the EDX spectrum, the chemical composition of the CaO nanoparticles was identified as shown in Fig. 4. This spectrum reveals that the minerals' elemental percentages (inset, Fig. 4), which confirmed the purity of the synthesized nano particles.

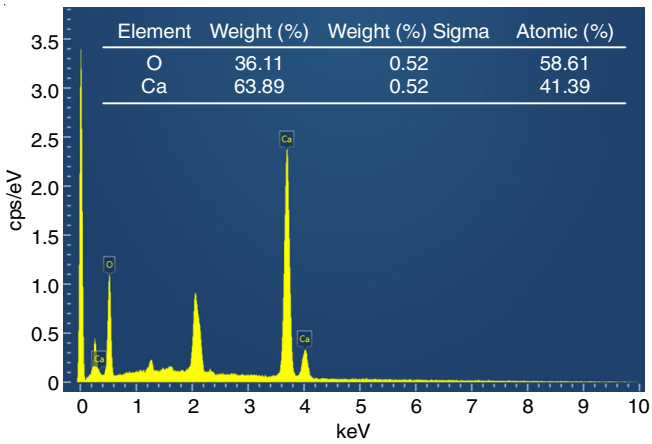

Fig. 4. EDX image of synthesized CaO nanoparticles using chicken eggshells

UV-visible studies: In this study, UV-visible spectra for CaO nanoparticles were obtained within the wavelength range of 260-400 nm (Fig. 5). The broad peaks were observed at 280 and 320 nm, indicating the formation of CaO NPs at these wavelengths. A sharp increase in absorption was detected at a wavelength of 360 nm, suggesting that CaO nanoparticles absorbed light in the ultraviolet spectrum [30].

FT-IR studies: FT-IR spectrum in the 4000-500 cm^{-1} range is displayed in Fig. 6 for CaO NPs. The band at 3416 cm^{-1} suggests the presence of absorbed water on the surface [31]. A sharp peak at 3419 cm^{-1} suggested the presence of alcohol

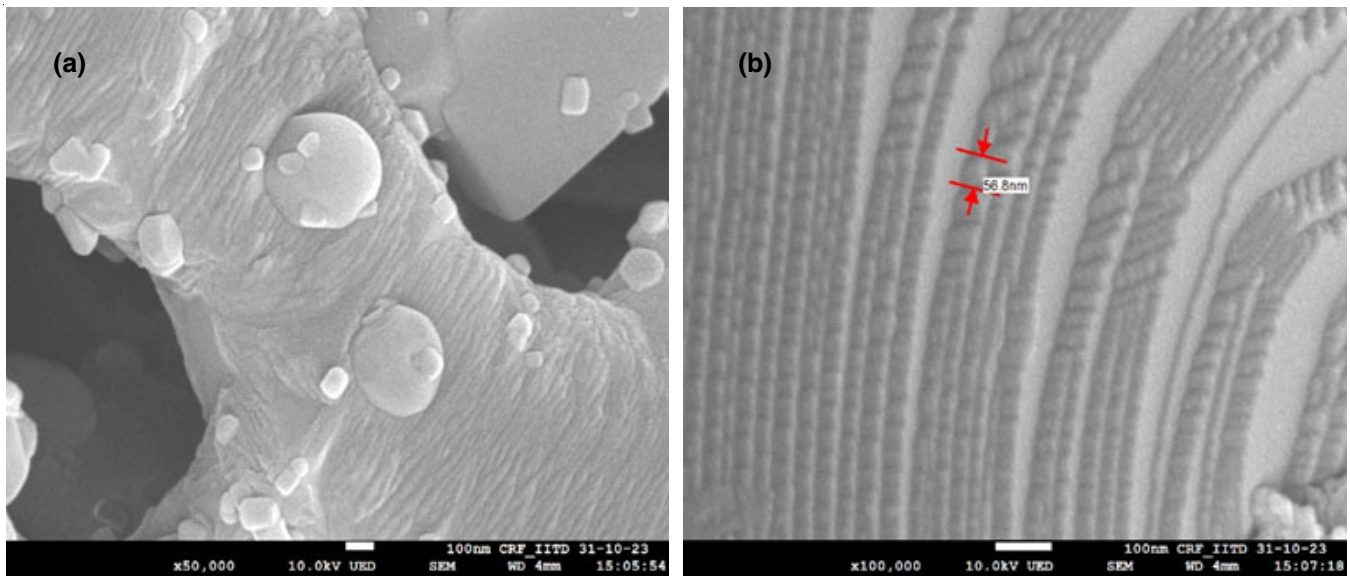

Fig. 3. SEM images of synthesized CaO nanoparticles using hen eggshells

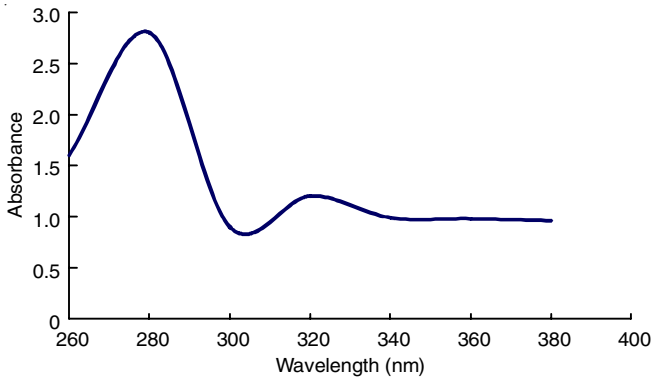

Fig. 5. UV-visible spectrum of synthesized CaO nanoparticles using hen eggshells

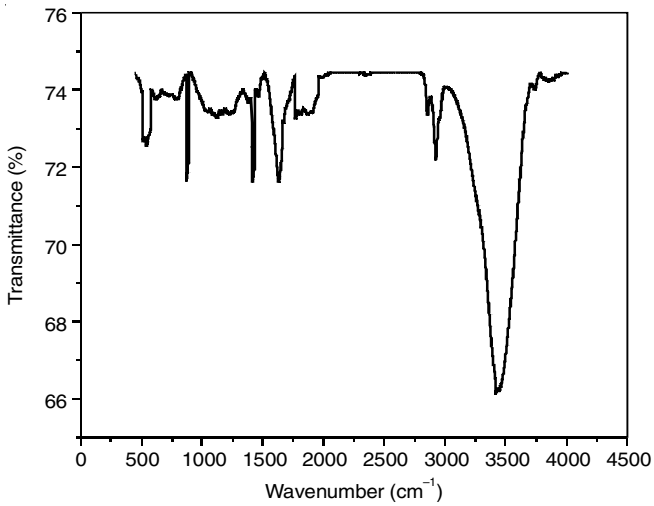

Fig. 6. FTIR spectra of synthesized CaO from hen eggshells

hydroxyl group and this absorption peak was noted in all the calcined samples [32]. The C=O stretching bonds were observed at 1632 and 1420 cm^{-1}, while the band at 554 cm^{-1} is due to the stretching of the Ca–O bonds.

Effects of synthesized CaO nanoparticles on *Chlorella* sp.: To evaluate the CaO nanoparticles effects on *Chlorella* sp., the *C. vulgaris* strain was cultivated in various doses of synthesized CaO NPs ranging from 0 to 30 mg L^{-1} within BG 11 medium. A progressive exponential growth occurred until 14th day after 20th day of batch study. The highest biomass concentration achieved 242.56 mg L^{-1} at 20 mg L^{-1}, whereas 220.53 and 112.21 mg L^{-1} recorded in 10 and 30 mg L^{-1} dose of CaO NPs (Fig. 7). The maximum specific growth rate and the highest biomass concentration for *C. vulgaris* were reached when egg-shell powder was added to the culture; these values were 2.25 g L and 0.453 per day, respectively [33].

Similarly, it was found that at a concentration of 20 mg L^{-1}, iron oxide nanoparticles (IONPs) demonstrated a maximum increase of 33.75% in biomass concentration over a 15-day cultivation period of *C. pyrenoidosa* [34]. The study examined that addition of SiO_2 nanoparticles to *C. vulgaris* resulted in a 177% growth in the biomass production [35]. It has been recorded that metal-based nanoparticles enhanced the growth parameters, including biomass production, specific growth rate, chlorophyll content, metabolites, *etc*. [36]. In contrast it has

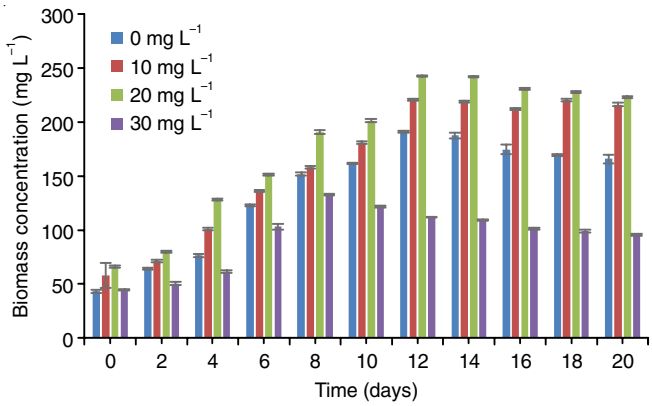

Fig. 7. Estimation of various doses of synthesized CaO nanoparticles on biomass concentration of *Chlorella* sp.

also observed that at lower concentration of nanoparticles can cause toxicity towards microalgae.

Similarly, chlorophyll-a content in *Chlorella* sp. shows an increasing pattern till 12th day. It was observed 16.81 µg mL^{-1} at 20 mg L^{-1} concentration. At doses of 30 and 20 mg L^{-1} of nano-CaO, the concentrations of chlorophyll-a were measured at 6.3 and 9.073 µg mL^{-1}, respectively (Fig. 8). In a study, DNA, chlorophyll and lipids were not released in significant amounts until the dosage of nickel nanoparticles reached 0.007 g/g of suspended solids (g/g SS), according to Kavitha *et al.* [37]. Above this limit, there was a sudden rise in DNA, lipids and chlorophyll (0.2 g/L, 0.8 µg/mL and 1.2 g/L, respectively). This suggested that the phospholipid bilayer of chloroplasts, which houses the green pigment chlorophyll, had been disrupted and that there had been cell lysis. This demonstrates unequivocally that disruption of biomass, dissolving of intracellular components and diffusion of chlorophyll from thylakoids into the surrounding aqueous phase occur when the dosage of nickel nanoparticles is greater than 0.007 g/g SS. Furthermore, the inoculation of 30 mg L^{-1} of Fe_2O_3 resulted in a 38% increase in carbohydrate content. However, a decrease in biomass concentration of 18% was observed due to the deposition of nanoparticles on the cyanobacteria cell wall [38]. The peak lipid yield of 35.71% occurred at a dosage of 20 mg L^{-1} CaO NPs, while 17.05% recorded at 0 mg L^{-1}. These fluctuations in growth

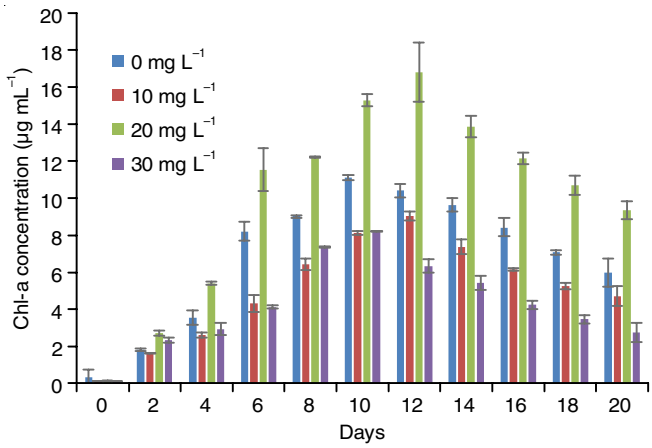

Fig. 8. Estimation of various doses of CaO nanoparticles on chlorophyll-a of *Chlorella* sp.

and lipid output signify the absorption of CaO nanoparticles and its effects.

In this study, it was observed that the lipid concentration in *Chlorella pyrenoidosa* increased by up to 16.89% (dry weight) upon the addition of 30 mg L^{-1} [34]. Similarly, it was reported that *C. vulgaris* exhibited a lipid increase of 39.7% and 25.5% when 50 and 100 mg L^{-1} of Fe_2O_3 NPs were introduced to the culture [39]. The transcriptome analysis showed the MCA1 upregulation and CAX/ACA1 down regulation, boosting cytoplasmic Ca^{2+}. The co-expression networks revealed Ca^{2+} fluctuation triggering MYB3 and AP2-4 *via* CAM and CDPK, modulating GPAT at TAG synthesis onset and DGAT/PDAT in the final stage [18]. In response to oxidative stress, the algae utilize antioxidant defence mechanisms, including the activation of reactive oxygen scavenging enzymes like catalase (CAT), superoxide dismutase (SOD), peroxidase (POD) and the synthesis of antioxidants such as carotenoids, ascorbic acid, proteins and sugars [40].

Conclusion

This study elucidated the phylogenetic relationship of a particular strain with *Chlorella* sp. and successfully synthesized calcium oxide nanoparticles (CaO NPs) from the waste hen eggshells, characterizing their properties through various analytical techniques. The evaluation of the green synthesized CaO NPs on *Chlorella* sp. revealed the promising results, with notable enhancements in biomass concentration, chlorophyll-a content and lipid yield at certain concentrations. However, caution is warranted as higher nanoparticle doses may induce toxicity, leading to adverse effects on cell growth and photosynthetic pigments.

CONFLICT OF INTEREST

The authors declare that there is no conflict of interests regarding the publication of this article.

REFERENCES

1. S.F. Ahmed, M. Mofijur, N. Rafa, A.T. Chowdhury, S. Chowdhury, M. Nahrin, A.B.M.S. Islam and H.C. Ong, *Environ. Res.*, **204**, 111967 (2022); https://doi.org/10.1016/j.envres.2021.111967
2. S. Bakand and A. Hayes, *Int. J. Mol. Sci.*, **17**, 929 (2016); https://doi.org/10.3390/ijms17060929
3. I. Hussain, N.B. Singh, A. Singh, H. Singh and S.C. Singh, *Biotechnol. Lett.*, **38**, 545 (2016); https://doi.org/10.1007/s10529-015-2026-7
4. N. Shreyash, S. Bajpai, M.A. Khan, Y. Vijay, S.K. Tiwary and M. Sonker, *ACS Appl. Nano Mater.*, **4**, 11428 (2021); https://doi.org/10.1021/acsanm.1c02946
5. A. Jayachandran, A.T.R and A.S. Nair, *Biochem. Biophys. Rep.*, **26**, 100995; https://doi.org/10.1016/j.bbrep.2021.100995
6. A. Gour and N.K. Jain, *Artif. Cells Nanomed. Biotechnol.*, **47**, 844 (2019); https://doi.org/10.1080/21691401.2019.1577878
7. R.S. Hamida, M.A. Ali, N. Mugren, M.I. Al-Zaban, M.M. Bin-Meferij and A. Redhwan, *ACS Omega*, **8**, 29169 (2023); https://doi.org/10.1021/acsomega.3c02368
8. D. Kulkarni, R. Sherkar, C. Shirsathe, R. Sonwane, N. Varpe, S. Shelke, S.R. Pardeshi, G. Dhaneshwar, V. Junnuthula, S. Dyawanapelly and M.P. More, *Front. Bioeng. Biotechnol.*, **11**, 1159193 (2023); https://doi.org/10.3389/fbioe.2023.1159193
9. V.P. Aswathi, S. Meera, C.G.A. Maria and M. Nidhin, *Nanotechnol. Environ. Eng.*, **8**, 377 (2023); https://doi.org/10.1007/s41204-022-00276-8
10. P.K. Dikshit, J. Kumar, A.K. Das, S. Sadhu, S. Sharma, S. Singh, P.K. Gupta and B.S. Kim, *Catalysts*, **11**, 902 (2021); https://doi.org/10.3390/catal11080902
11. S. Jadoun, R. Arif, N.K. Jangid and R.K. Meena, *Environ. Chem. Lett.*, **19**, 355 (2021); https://doi.org/10.1007/s10311-020-01074-x
12. I. Ijaz, E. Gilani, A. Nazir and A. Bukhari, *Green Chem. Lett. Rev.*, **13**, 223 (2020); https://doi.org/10.1080/17518253.2020.1802517
13. P. Kaushik and A. Chauhan, *Indian J. Microbiol.*, **48**, 348 (2008); https://doi.org/10.1007/s12088-008-0043-0
14. S. Zhang, L. Zhang, G. Xu, F. Li and X. Li, *Front. Microbiol.*, **13**, 970028 (2022); https://doi.org/10.3389/fmicb.2022.970028
15. K. Thor, *Front. Plant Sci.*, **10**, 440 (2019); https://doi.org/10.3389/fpls.2019.00440
16. E. Hoiczyk and A. Hansel, *J. Bacteriol.*, **182**, 1191 (2000); https://doi.org/10.1128/JB.182.5.1191-1199.2000
17. C.-C. Tang, X.-Y. Zhang, R. Wang, T.-Y. Wang, Z.-W. He and X.C. Wang, *Environ. Res.*, **207**, 112228 (2022); https://doi.org/10.1016/j.envres.2021.112228
18. J. Yang, W. Li, C. Xing, G. Xing, Y. Guo and H. Yuan, *Environ. Res.*, **208**, 112696 (2022); https://doi.org/10.1016/j.envres.2022.112696
19. A. Farooq, S. Javad, K. Jabeen, A. Ali Shah, A. Ahmad, A. Noor Shah, M. Nasser Alyemeni, W. F.A Mosa and A. Abbas, *J. King Saud Univ. Sci.*, **35**, 102647 (2023); https://doi.org/10.1016/j.jksus.2023.102647
20. Y. Mbenga, M.S. Mthana, D.M.N. Mthiyane, O.E. Ogunjinmi, M. Singh and D.C. Onwudiwe, *Inorg. Chem. Commun.*, **151**, 110581 (2023); https://doi.org/10.1016/j.inoche.2023.110581
21. G. Marquis, B. Ramasamy, S. Banwarilal and A.P. Munusamy, *J. Photochem. Photobiol. B*, **155**, 28 (2016); https://doi.org/10.1016/j.jphotobiol.2015.12.013
22. J. Arora, A. Ranjan, A. Chauhan, V.D. Rajput, S. Sushkova, E.V. Prazdnova, T. Minkina, R. Biswas, S. Joshi, T. Jindal and R. Prasad, *Appl. Biochem. Biotechnol.*, (2023); https://doi.org/10.1007/s12010-023-04647-y
23. S. Kumar, G. Stecher, M. Li, C. Knyaz and K. Tamura, *Mol. Biol. Evol.*, **35**, 1547 (2018); https://doi.org/10.1093/molbev/msy096
24. A. Chauhan and T. Jindal, Microbiological Methods for Environment, Food and Pharmaceutical Analysis, Springer Nature (2020).
25. O. Awogbemi, F. Inambao and E.I. Onuh, *Heliyon*, **6**, e05283 (2020); https://doi.org/10.1016/j.heliyon.2020.e05283
26. S.L. Nielsen and B.W. Hansen, *Aquacult. Res.*, **50**, 2698 (2019); https://doi.org/10.1111/are.14227
27. R.J. Porra, W.A. Thompson and P.E. Kriedemann, *Biochim. Biophys. Acta Bioenerg.*, **975**, 384 (1989); https://doi.org/10.1016/S0005-2728(89)80347-0
28. E.G. Bligh and W.J. Dyer, *Can. J. Biochem. Physiol.*, **37**, 911 (1959); https://doi.org/10.1139/y59-099
29. K. Gaurav, S. Kumari and J. Dutta, *J. Biochem. Technol.*, **12**, 49 (2021); https://doi.org/10.51847/eqTib7hM7Z
30. S. Kumar, V. Sharma, J.K. Pradhan, S.K. Sharma, P. Singh and J.K. Sharma, *Nano Biomed. Eng.*, **13**, 172 (2021); https://doi.org/10.5101/nbe.v13i2.p172-178
31. M.-M. Pedavoah, M. Badu, N.O. Boadi and J.A.M. Awudza, *Green and Sustainable Chem.*, **08**, 208 (2018); https://doi.org/10.4236/gsc.2018.82015
32. M.S. Tizo, L.A.V. Blanco, A.C.Q. Cagas, B.R.B. Dela Cruz, J.C. Encoy, J.V. Gunting, R.O. Arazo and V.I.F. Mabayo, *Sustain. Environ. Res.*, **28**, 326 (2018); https://doi.org/10.1016/j.serj.2018.09.002

33. H.J. Choi, *Biotechnol. Biotechnol. Equip.*, **29**, 666 (2015); https://doi.org/10.1080/13102818.2015.1031177
34. M.S. Rana, S. Bhushan, D.R. Sudhakar and S.K. Prajapati, *Algal Res.*, **49**, 101942 (2020); https://doi.org/10.1016/j.algal.2020.101942
35. H.-S. Jeon, S.E. Park, B. Ahn and Y.-K. Kim, *Biotechnol. Bioprocess Eng.*, **22**, 136 (2017); https://doi.org/10.1007/s12257-016-0657-8
36. M.K. Kanwar, S. Sun, X. Chu and J. Zhou, In: A. Husen and M. Iqbal, Impacts of Metal and Metal Oxide Nanoparticles on Plant Growth and Productivity, In: Nanomaterials and Plant Potential, Springer International Publishing, pp. 379-392 (2019).
37. S. Kavitha, M. Schikaran, R.Y. Kannah, M. Gunasekaran, G. Kumar and J.R. Banu, *Bioresour. Technol.*, **289**, 121624 (2019); https://doi.org/10.1016/j.biortech.2019.121624
38. L. Vargas-Estrada, P.U. Okoye, R. Muñoz, E. Novelo Maldonado, A. González-Sánchez and P.J. Sebastian, *Algal Res.*, **78**, 103399 (2024); https://doi.org/10.1016/j.algal.2024.103399
39. M. Bibi, X. Zhu, M. Munir and I. Angelidaki, *Chemosphere*, **282**, 131044 (2021); https://doi.org/10.1016/j.chemosphere.2021.131044
40. M.M.S. Ismaiel and M.D. Piercey-Normore, *Environ. Pollut.*, **341**, 123002 (2024); https://doi.org/10.1016/j.envpol.2023.123002